ilmedia

TECHNISCHE UNIVERSITÄT
ILMENAU

Seibold, Marc; Schricker, Klaus; Bergmann, Jean Pierre

Systematic adjustment of the joining time in pulsed laser beam welding of aluminum-copper joints by means of a closed-loop control

Original published in: Journal of advanced joining processes. - Amsterdam : Elsevier. - 5 (2022), art. 100104, 6 pp.

Original published: 2022-02-05

ISSN: 2666-3309

DOI: 10.1016/j.jajp.2022.100104

[*Visited:* 2022-05-11]

This work is licensed under a Creative Commons Attribution 4.0 International license. To view a copy of this license, visit https://creativecommons.org/licenses/by/4.0/

TU Ilmenau | Universitätsbibliothek | ilmedia, 2022
http://www.tu-ilmenau.de/ilmedia

Journal of Advanced Joining Processes 5 (2022) 100104

Contents lists available at ScienceDirect

Journal of Advanced Joining Processes

journal homepage: www.sciencedirect.com/journal/journal-of-advanced-joining-processes

Systematic adjustment of the joining time in pulsed laser beam welding of aluminum-copper joints by means of a closed-loop control

M. Seibold *, K. Schricker, J.P. Bergmann

Production Technology Group, Technische Universität Ilmenau, Gustav-Kirchhoff-Platz 2, 98693 Ilmenau, Germany

ARTICLE INFO

Keywords:
Pulsed laser beam welding
Closed loop control
Aluminium-copper joints
Tensile shear force
Process emission
Half section welding

ABSTRACT

Electric mobility has become increasingly important in recent years. For this purpose, the use of copper is essential due to its electrical properties. In order to save weight and costs, copper is replaced by aluminum in many electrical conductors.In this paper, the required joining time for pulsed laser beam welding of aluminum-copper joints is investigated to minimize the mixing of both materials. By using an external controller and photodiodes, it was possible to develop a real-time pulse control laser welding process based on process emissions. The spectral emission was used to detect when the lower joining partner is reached during the deep welding process. The control enables the adjustment of different joining times, on the one hand by a signal drop of the spectral emission, on the other hand by a specific time. The laser pulse was terminated between 500 – 800 µs after reaching this event. This led to differences in process conditions, resulting in significant changes in mechanical properties. In this way, a decisive influence was exerted on the resulting joining zone. The interaction duration and the work piece transition are of primary interest. By comparing the results with high-speed recordings in the half-section set-up, the resulting mechanisms can be identified. It could be shown that the breakup time have an high impact for the shear tensile force and the welding depth. A Change in the breakup time of 40 µs could lead to high changes in the tensile shear force.

Introduction

The combination of lightweight construction and electrical engineering has become much more relevant in the past few years. The reason for this is the increasing interest in e-mobility. (press office 2021) The weight increases due to battery in an electric car. The reason for this is the weight of materials that are used to transmit electricity. Copper is a common electrical conductor and has a higher density than steel. Therefore, this material is replaced more and more by aluminum. The lower price and the lower density with the same electrical conductivity is the reason for this substitution. (press office 2021; Bergmann et al., 2013) The replacement of copper with aluminum cannot happen completely. Aluminum forms an oxide layer at the surface, that has an electrically isolating effect and is particularly relevant for connector terminals. Therefore, copper alloys are used at the contact surfaces. For this reason, manufacturing of aluminum-copper joints is essential for addressing lightweight construction and electrical properties at the same time. The solubility of copper in aluminum and vice versa is limited at room temperature and intermetallic compounds are formed during welding over melting temperature due to the mixing of both materials. The intermetallic compounds are superstructures and characterized by a very high electrical resistance and high brittleness compared to the base materials. (Braunovic and Aleksandrov, 1992; Hyoung-Joon et al., 2003) Typically aluminum material used was a pure aluminum of the type EN AW-1050A that is considered weldable. For the copper material, the alloy EN CW004A was used, an alloy with a residual oxygen content and poor welding properties. (Hofmann et al., 2014)

Joining aluminum and copper by using a laser beam source presents some challenges to the joining process. The large differences in absorption at typical solid-state laser wavelengths in the near infrared range leads to large fluctuations in depositing laser beam power. The absorptivity of aluminum at 1 µm wavelength is approx. 10%, that of copper aprox. 2% (Sakagawa et al., 2011). This behavior requires high intensities for processing copper (Heider et al., 2011). Since the lap joint is of great relevance for many applications, aluminum is chosen as the upper joining partner due to its higher absorption coefficient. To reduce the amount of intermetallic compounds in pulsed welding process, the lower joining partner should be minimally melted in order to control or

* Corresponding author.
E-mail address: marc.seibold@tu-ilmenau.de (M. Seibold).

https://doi.org/10.1016/j.jajp.2022.100104
Received 12 November 2021; Received in revised form 27 January 2022; Accepted 27 January 2022
Available online 29 January 2022
2666-3309/© 2022 The Author(s). Published by Elsevier B.V. This is an open access article under the CC BY license (http://creativecommons.org/licenses/by/4.0/).

limit intermixing in the molten area. Thereby, a strong imbalance between both molten materials can be achieved, leading to a reduced formation of intermetallic compounds because more copper can be dissolved regarding the phase diagram of copper and aluminum. (Massalski, 1980) In order to address the minimal melting of copper, pulsed laser welding is a possible approach. The energy put of each pulse affects the amount of melted material, the mixing between aluminum and copper and the penetration depth within the lower joining partner, typically copper. However, the energy input of each pulse is strongly deviating due to unstable conditions of the keyhole during the aluminum-copper welding process. (Mys and Schmidt, 2006) These instabilities of the process can be determined by the spectral process emissions. Photodiodes allow a fast detection of emission signals that cannot be achieved by spectrometers. (Opto Semiconductors GmbH, 2014; Avantes solutions in spectroscopy 2013)

Therefore, photodiodes targeted to the process zone are used to record the spectral process emissions (Schmalen and Plapper, 2018; Seibold et al., 2020; Eriksson et al., 2009). Fig. 1 shows the photodiode voltage and the laser power for an aluminum-copper weld in overlap configuration. The red line shows the set laser power that is given by the analog-digital converter as an analog signal. The black curve corresponds to the output laser power which is provided by the laser beam source directly due to an analog voltage signal. The power threshold of the laser beam source causes a small time delay until beam power is provided (approx. 0.8 ms). For all welds, a rising ramp was used as the pulse shape. The continuous power increase has advantages over a rectangular pulse shape in terms of spatter formation and temporal resolution of process stages for the controlled process (heat conduction welding, deep welding). The gray curve represents a photodiode signal of the process emission at a wavelength of 485 nm which is used as controlled variable. This characteristic signal course is reproducible for the pulsed laser welding process (press office 2021). Characteristic points during the welding process are shown additionally. Point ① correlates the heat conduction welding process before a keyhole is formed. Followed by point ②, that represents the beginning of the deep welding process. Due to the increase in evaporating material, the emission also increases and thus the photodiode voltage. The signal increases up to point ③ and then drops significantly. This signal maximum correlates when the lower joining partner is reached by the keyhole. Previous publications showed that this significant signal curve can be found for various material combinations and that a closed-loop control can be built up on this basis. (press office 2021; Avantes solutions in spectroscopy 2013) It can be concluded that the photodiode's voltage signal correlates to the process stages which is why it can be implemented as control variable in a closed-loop control. (Mathivanan and Plapper, 2019) A controlled process would offer advantageous in order to detect the interface between aluminum and copper reliably. (Avantes solutions in spectroscopy 2013) Such a control was implemented based on the spectral process emissions recorded by photodiodes. (Avantes solutions in spectroscopy 2013)

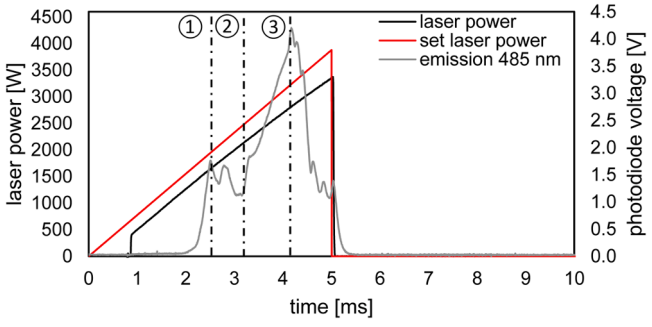

Fig. 1. Signal course of the deep welding process of aluminum and copper in overlap configuration.

The Fig. 2 shows the schematic principle of the control strategy used. The gantry control triggers the control system. The control unit used is an ADWin-Pro II system from Jäger Messtechnik. Its analog-digital converter allows cycle frequencies of up to 1 GHz. In this process the cycle time is limited to 5 µs. The cycle time enables a real-time ability of the control system and is twice as fast as the cycle time of the beam source's power supply. The control system loops the "set laser power"-signal - through to the laser beam source and additionally generates the laser pulse signal to the analog input of the laser beam source. The laser beam source takes the analog voltage signal and converts it into laser power which is emitted. Because the control system regulates the pulse shape, the pulse generation is not done by the beam source. With the analog output of the laser beam source becomes the diode voltage of the laser beam source is ground back. This signal is recorded by the controller and can later be used for comparison with the set power value. In the following, this signal is referred as "laser power" or, in the case of closed-loop control, as "controlled laser power". The beam source provides laser power based on the value of the analog input, resulting in spectral process emission due to interaction between laser beam and materials. The signal of process emissions picked up by the photodiodes is used as controlled variable, amplified and coupled to the control system. On the basis of these emissions, the laser pulse can be changed until the next cycle of the laser beam source. Therefore, an in-process control of laser beam power is possible. In this publication, power breakups to zero watt are presented at different points in time. Thereby a detailed understanding of different interaction times at the boundary surface and their effects to the welded joint shall be considered in this work.

Experimental setup

For the detection and control of the welding process, some limits in the experimental setup must be set. The selected photodiodes, type BPW 21, have an operating range of wavelengths between 350 nm and 820 nm and a maximum sensitivity at 500 nm, that makes them suitable for detection of spectral process emissions in the visible spectrum. Overexposure of the photodiodes is prevented by a bandpass filter mounted in front. An attenuation of the exposure is the only limitation. This can be done by a density filter or, as in this case, by a bandpass filter. Due to the aluminum material EN AW-1050A as upper joining partner, a bandpass filter with a wavelength of 485 nm and full widthwidth half maximum of 20 nm has been chosen. If a different filter is used, the signal gain would have to be adjusted. The welding was performed with a beam source from the company IPG Photonics of the type YLR-450/4500-QCW (wavelength: 1070 nm, maximum beam power in pulsed wave mode: 4500 W). The laser beam source uses a fast-working power supply for the laser diodes used for pumping the active fiber. Normal power supplies in laser beam sources have a cycle time of 50 µs and are therefore 5 times slower than those of the beam source used in this study. The processing optic FLW D30 is also from IPG Photonics an equipped with a collimator lens of 85 mm and a focusing lens of 200 mm. With the used light guide cable of 200 µm diameter, the calculated focus diameter is 470 µm. The focus position was placed on the workpiece surface. The processing optic is mounted on a 3-axis-gantry to carry out line welds or single pulses. The Figure below shows the control of a single pulse with the described setup.

Two different breakup controls are investigated based on the closed-loop control developed in (press office 2021; Heider et al., 2011) that allow the control of laser beam power in each pulse. The differences in these strategies are shown in Fig. 3. Again, the black curve represents the laser power output by the beam source and the gray curve corresponds to the measured process emission at wavelength 485 nm. The dashed line represents the pulse shape of the uncontrolled process. The process control allows two possible approaches for realizing a breakup control, i. e. to interrupt the laser output power. After reaching the second peak which indicates the boundary layer between both materials, either the

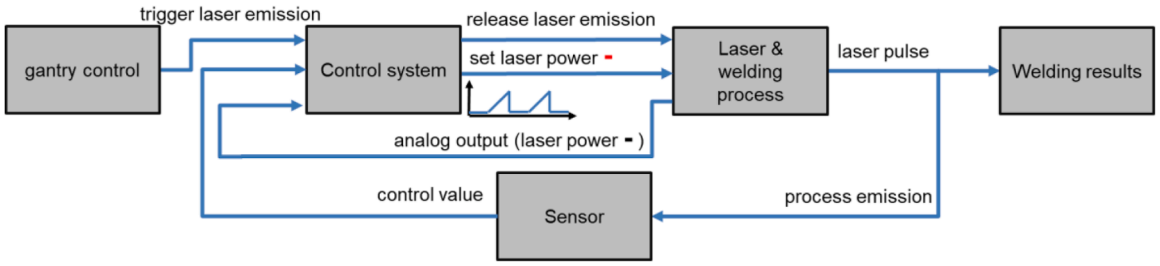

Fig. 2. schematic principle of the used close-loop control.

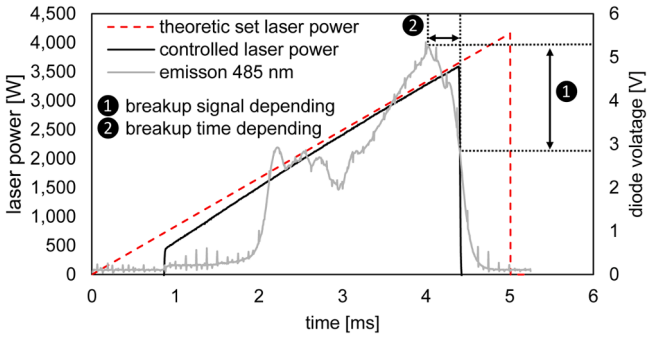

Fig. 3. Signal course of the an controlled deep welding process.

signal drop can be controlled by a previously defined value ❶ or to a defined time period ❷. To better visualize this behavior, single pulse welds were done in a half-section configuration.

In order to show that the signal maximum correlates with reaching the keyhole of the lower joint partner ③, single spot welds were carried out in the half-section process in addition to the pulsed line welds. Fig. 4 shows a schematic illustration of the set-up. Similar to line welds, aluminum (EN AW-1050A) and copper (EN CW004A) were welded in an overlap configuration. Single-pulse welds were performed to provide a better understanding of the keyhole behavior during welding. A borosilicate glass pane from Schott (Borofloat 33) was positioned on the edge of the overlap configuration. The edge is facing the glass which was over-milled to minimize the air cavity between the glass surface and both materials. The laser spot was positioned half on the workpiece surface and half on the glass. The Highspeed camera Photron SA – X2 was used with a frame rate of 50,000 fps for imaging in order to resolve the different stages of the welding process over time. To eliminate the wavelength of the laser beam source for the recordings, a blocking filter

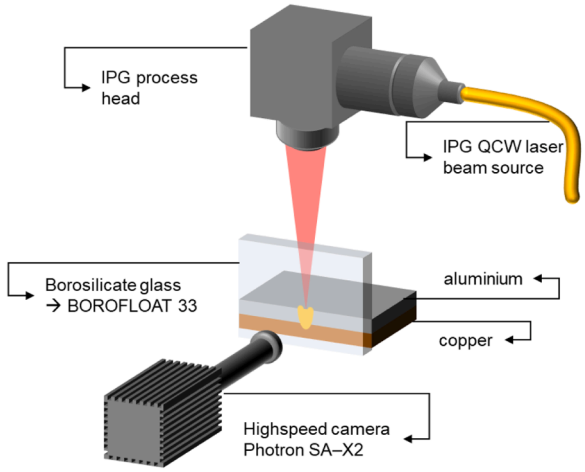

Fig. 4. Schematic illustraction of the set-up.

(NF 1064 −44 nm) is mounted in front of the camera.

Single-pulse welds provide small contact areas between aluminum and copper and therefore a limited meaningfulness in terms of mechanical characterization. For this reason, line welds have been created, as this is a summation of several individual pulses. The feed rate is set to 1 m/min. Due to the repetition rate of the beam source, the pulse overlap is set to prevent that the nominal focus diameters overlap. This procedure allows the keyhole to impinge a non-melted interface between aluminum and copper during joining. It should be noted that the high thermal conductivity of aluminum leads to overlapping melt pools at the top surface of the weld seam whereas the connection between both materials is not continuous at the boundary layer. To generate artificial aging in the line welds, the welded samples were then heated in a muffle furnace. The exact procedure is explained in the following chapter.

Results and discussion

In order to illustrate the welding process for the single pulses, the results of the half-section process will be addressed first. The photodiode signals of the spectral process emission correlates with different process stages, e.g. reaching the lower joining partner at the peak value as shown before in Fig. 1. In order to develop a deeper understanding of the processes at the interface between both joining partners, investigations in a half-section setup were carried out.

Fig. 5 assigns the laser power to specific frames from high-speed images. On the left side of the illustration, the set and output laser power is shown over time. In addition, the time points are listed which can be found on the right side of the illustration. The snapshots of the

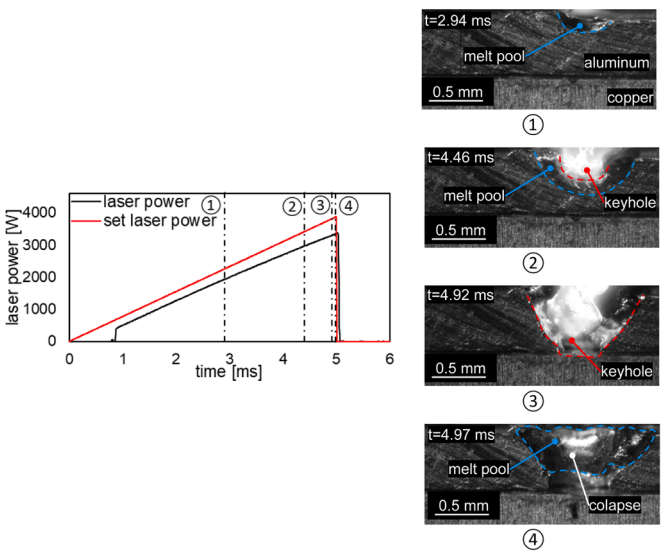

Fig. 5. left: set laser power and real laser output. Right: single frames of the half-section process at different time steps. ① beginning of the heat conduction welding process. ② beginning of the deep welding process. ③ Keyhole reaches the lower joining partner. ④ collapse of the keyhole.

high-speed images show the key points of the process during a single pulse. Because of the glass pane, the flow conditions are altered and the keyhole is opened towards the high-speed camera, which is why radiation conditions of spectral process emission are significantly compared to the regular process. For this reason, no spectral process emissions could be recorded during investigations in half-section setup. Frame ① shows the beginning of the heat conduction welding after 2.94 ms. The melt pool can be identified within the red dashed line. In frame ② the beginning of the deep welding process is depicted. The bright area on top can clearly be identified as the keyhole (Tenner et al., 2018). In the last frame ③, the keyhole reaches the lower joining partner. At this point, the lower joining partner was not yet melted, but the keyhole does not exceed the boundary layer between both materials. The keyhole diameter increases as a result, which influences the flow condition of the metal vapor stream. At this time step the welding depth is no more longer rising and the keyhole starts to collapse ④. Due to the glass pane, the rest melt flows from the back of the glass pane towards it. In welds without a half-section configuration, the molten metal would flow together radially and close the keyhole. Due to the continuous energy input during a pulse, more energy is deposited and the keyhole opens again and melting of the lower joining begins. In the diode signal of Fig. 2 it can be seen that after the signal maximum, the value of the diode voltage drops to the value of the heat conduction welding of the beginning. This can be explained by the collapse of the keyhole. Since there is no more a keyhole at the time of the collapse, the flow conditions are the same as those of the heat welds. The changed coupling conditions of the laser beam have led to the switch from heat conduction welding to deep penetration welding at a later time of the pulse.

The detection of the interface, in combination with the control system setup, enables the adjustment of the mixing between aluminum and copper. As shown in section 2, the breakup control can be implemented in two ways. The first method controls the drop of the diode voltage signal by a set value. The set value was varied from 4.5% to 30% voltage drop. A regulation on a larger signal drop, over 30% could lead to the fact that the breakup does not happen. The signal drop after the maximum does not drop to zero but to a value similar to that of heat conduction welding ①. In this case, the difference between the maximum photodiode voltage and the photodiode voltage value of the heat conduction welding would not be large enough for the closed-loop control to react. The second breakup control is based on a set time value that must be passed after reaching the photodiode voltage maximum until the laser power is stopped. The set time value was varied from 0.3 ms to 0.8 ms. Investigations with the two control strategies are implemented by line welds consisting of 50 individual pulses and a distance between each pulse of 0.5 mm. The resulting weld was then evaluated in tensile-shear tests. For statistical validation, each weld was carried out 5 times, resulting in 250 evaluable individual pulses in total.

For a better visualization of the control strategy, the above Fig. 6 show time-dependent controlled signal curves. Three different breakup times of 0.3 ms a), 0.5 ms b) and 0.7 ms c) were shown. Across all depicted breakup times, a similar behavior of the emission signal was determined. Since the signal maximum appears at comparable times for each pulse, the absolute pulse length is extended by the length of the termination time approximately. Over all breakup parameters it can be seen that the power drop if the laser beam source (black) minimally follows the signal drop of the controller (red). This deviation reasons in the different cycle times of the laser beam source and controller. The value ranges between 5µs and 10 µs. It can be seen that the control of different breakup times can be set reproducibly and therefore there is comparability in mechanical testing like shear tensile test.

In Fig. 7, both different breakup controls are summarized. Because the joining zone was carried out in overlap configuration, tensile-shear tests were carried out. The tensile-shear force is plotted on the vertical axis and no stress was calculated due to the hardly determinable bending moment and connected area between both materials. On the horizontal axis the breakup time is displayed. In order to include the tests with the

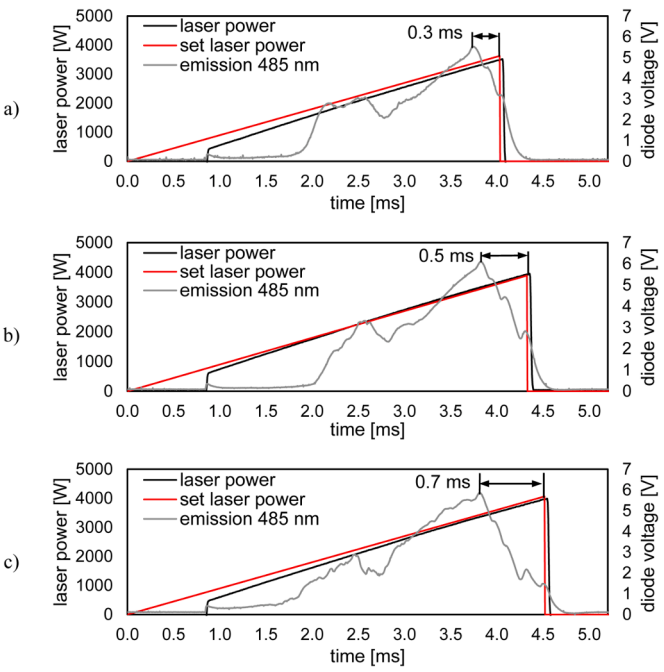

Fig. 6. time-depending breakup control ❷ of an aluminum copper welding with several time steps. a) breakup time of 0.3 ms after diode signal maximum. b) breakup time of 0.5 ms after diode signal maximum. c) breakup time of 0.7 ms after diode signal maximum.

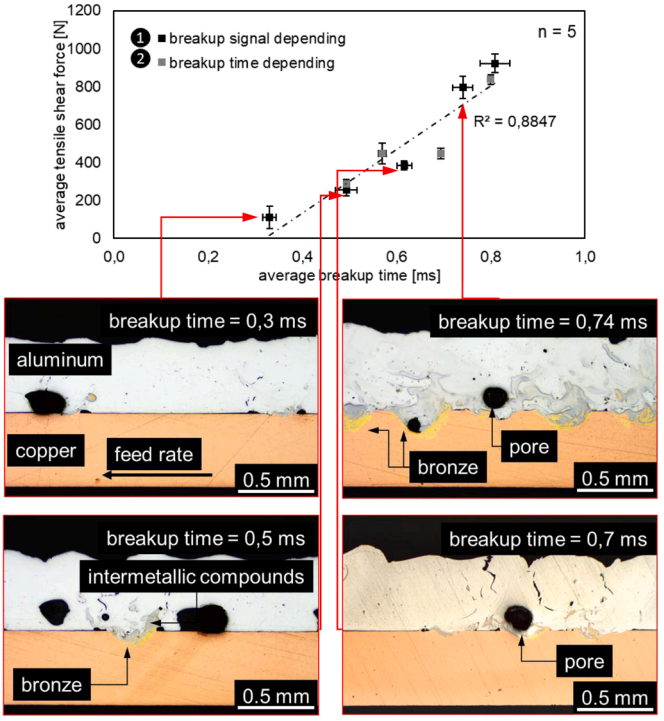

Fig. 7. Comparison of the control strategies used in relation to the average tensile force and breakup time. As well as longitudinal microsections at different breakup times.

ignal-dependent breakup control and to make them comparable, the breakup time was measured based on the recorded data. Therefore, the times between the signal maximum and the power reduction were determined. It is of interest for the process control, that the fluctuation of signal drop duration can be classified as rather small, e.g. ± 0,1 ms. It

can be assumed that the signal drop correlates with the collapse of the keyhole and it follows that keyholes of various welds collapse at comparable times after reaching the interface between aluminum and copper. Because the second control strategy is about concrete times that are set for the power reduction, the horizontal error bars are close to zero. Regardless of the control strategy used, a linear trend with a degree of determination for all parameters ($R^2 = 0{,}8847$) can be seen. This trend shows that increasing contact time at the joint area leads to rising tensile-shear forces. The reason is the increase of melted material and therefore the increase of the contact area between aluminum and copper. This can be seen very well in the longitudinal microsections. At short breakup times such as 0.3 ms, the aluminum material is minimally molten and very sporadically it is coupled into the copper material. With the increase of the breakup times, the shear tensile force increases and it is coupled into the copper material in more places. With increasing breakup time and thus increasing time of interaction between keyhole and copper at the surface interface, the weld penetration depth into the lower joining partner increases. At the same time, the mixing of both materials increases leading to an increase in the intermetallic compounds which becomes apparent in the microsection through the formation of bronzes. What really stands out here is the change from 0.7 ms to 0.74 ms. The small increase in breakup time leads to a strong increase in shear force. In the comparison of the microsections, it can be seen that deep welding into copper takes bigger place at 0.74 ms and this doesn't happen at 0.7 ms. The shear tensile force is also increased. It can be noticed that at a breakup time of 0.7 ms less aluminum bronze and intermetallic compounds are to recognize than at a breakup time of 0.74 ms.

In order to check if there are less intermetallic compounds or if they are just not visible, the welds were tempered and then tensile shear tested. In this process, the sample was tempered in the muffle furnace at 400 °C for 60 minutes to induce an artificially aging process. If the mixing is strong, the diffusion in the weld seam may increase when the sample is tempered. In the welds with a strong mixing, there is more potential for an increase in intermetallic compounds. The basic approach is that intermetallic compounds grow thicker and therefore the tensile force is estimated to drop.

Fig. 8 shows the results from the artificially aged welds. In Fig. 8a) and b), the squares correspond to welds that were tested mechanically immediately after welding and the triangles to welds that were tempered before mechanical testing. The continuous lines is the linear regression line of the non-tempered samples and the dashed lines correspond to the tempered samples. In case of time-dependent tempered welds with a breakup time of 0.3 ms, no tensile tests could be carried out because these samples separated without the influence of an external force. The influence on the tensile shear force due to the tempering is higher. The decrease in tensile force with increasing breakup time is higher for the time-dependent controlled welds than for those with the signal decrease. A direct comparison between the tempered and non-tempered welds with a breakup time of 0.7 ms shows that no large amount of intermetallic compounds has formed. The deformation path couldn't use as a comparison parameter because the main influence of the welding comes from base material. This can be seen in the comparison between the tempered welds and the non-tempered welds. At a breakup time of 0.7 ms, the tensile shear force is nearly the same but the deformation path increases by twice the line. The dark gray area, which corresponds to the intermetallic compounds, did not grow further in the close-up images 1 and 2 due to the tempering. This shows that fewer intermetallic compounds were formed in these welds, which is why the stress drop is also lower for these parameters. It can therefore be established that coupling into copper is essential for shear strength, but that this must only be done minimally.

Conclusion

In this paper, it was shown by the half-section experiment that the

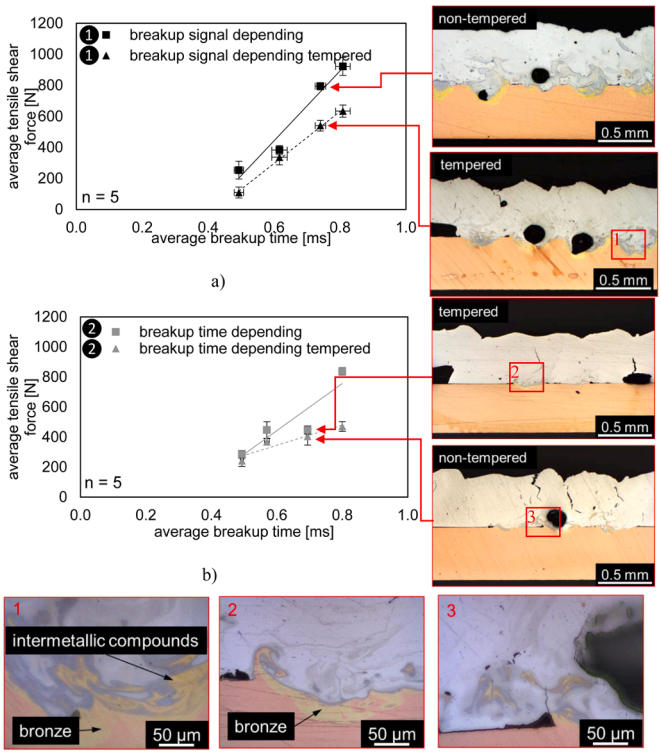

Fig. 8. Comparison of the tensile shear force of the tempered and non-tempered, that can be tolerated versus the interaction duration. a) for the signal depending breakups. b) for the time depending breakups.

diode signal waveform has a causal correlation in a pulsed laser welding in overlap configuration. Thereby, the detection of the boundary layer between the two materials is possible. A closed loop control on this interface could be generated. In order to investigate the influence of the connection more closely, two control strategies were demonstrated as well as their impact on the achievable tensile force. It was found that with increasing deposited power in the contact area, a larger bonding area and intermixing takes place. This is especially apparent with high breakup time of more than 0.7 ms. This is of primary relevance for the tensile strength, which is why the tensile force increases with increasing of the breakup time. In addition, it could be shown that small changes in the breakup time of 40 µs lead to large changes in the welding depth and mixing. This fact again shows the necessity of a control and the use of a power supply with a cycle time of 10 µs.

Declaration of Competing Interest

The authors declare that they have no known competing financial interests or personal relationships that could have appeared to influence the work reported in this paper.

Acknowledgements

We thank the Federal Ministry for Economic Affairs and Energy (BMWi) within the Zentrales Innovationsprogramm Mittelstand (ZIM) for funding the project. (FKZ 16KN053046)

References

press office, First global e-mobility ranking, https://www.vda.de/en/press/press-releases/210423-First-global-e-mobility-ranking.html, 2021.
press office, Comparison of Aluminium and Copper, https://www.alcunnect.de/Vergleich-Aluminium-und-Kupfer?language_id=3, 2021.
Bergmann, J.P., Petzoldt, F., Schürer, R., Schneider, S., 2013. Solid-state welding of aluminum to copper—case studies. Welding in the World. Volume 57, 541–550.

Braunovic, M., Aleksandrov, N., 1992. Intermetallic Compounds At Aluminum-To-Copper and Copper-To-Tin Electrical Interfaces. IEEE, pp. 25–34.
Hyoung-Joon, K., et al., 2003. Effects of Cu/Al intermetallic Compound (IMC) On Copper Wire and Aluminum Pad Bondability, 26. IEEE, pp. 367–374.
Hofmann, K., Holzer, M., Hugger, F., Roth, S., Schmidt, M., 2014. Reliable copper and aluminum connections for high power applications in electromobility. Phys. Procedia 56, 601–609.
Sakagawa, T., Nakashiba, S., Hiejima, H., 2011. Laser micro welding system and its application to seam welding of rechargeable battery. Phys. Procedia 12, 6–10.
Heider, A., Stritt, P., Hess, A., Weber, R., Graf, T., 2011. Process stabilization at welding copper by laser power modulation. Phys. Procedia 12, 81–87.
Massalski, T.B., 1980. The Al−Cu (Aluminum-Copper) system. Bull. Alloy Phase Diagrams 1, 27–33.
Mys, I., Schmidt, M., 2006. Laser micro welding of copper and aluminum, laser-based micropackaging. Proc. Vol. 6107.
O.S.R.A.M. Opto Semiconductors GmbH, Silicon photodiode for the visible spectral range (BPW 21), 2014.
Avantes solutions in spectroscopy, AVASOFT for AvaSpec-USB2 version 7.8 USER'S MANUAL, 2013.
Schmalen P., Plapper P., Spectroscopic studies of dissimilar Al-Cu laser welding manufacturing, sicence and engineering conference, 2018.
Seibold, M., Friedmann, H., Schricker, K., Bergmann, J.P., 2020. Process control by real-time pulse shaping in laser beam welding of different material combinations. Procedia CIRP 94, 769–774.
Eriksson E.A.I., Norman, P. Kaplan, A.F.H., Basic study of photodiode signals from laser welding emissions, 2009.
Mathivanan, K., Plapper, P., 2019. Laser welding of dissimilar copper and aluminum sheets by shaping the laser pulses. Procedia Manuf. 36.
Tenner, F., Eschner, E., Benjamin, L., Schmidt, M., 2018. Development of a joining gap control system for laser welding of zinc-coated steel sheets driven by process observation. J. Laser Appl. 30.